Am J Physiol Lung Cell Mol Physiol 289: L750–L759, 2005;
doi:10.1152/ajplung.00151.2005.

GXD/A+P/GO

J104973

Stage-specific regulation of respiratory epithelial cell differentiation by Foxa1

V. Besnard,[1] S. E. Wert,[1] K. H. Kaestner,[2] and J. A. Whitsett[1]

[1]*Department of Pediatrics, Division of Pulmonary Biology, Cincinnati Children's Hospital Medical Center and University of Cincinnati College of Medicine, Cincinnati, Ohio; and* [2]*Department of Genetics, University of Pennsylvania School of Medicine, Philadelphia, Pennsylvania*

Submitted 5 April 2005; accepted in final form 22 June 2005

Besnard, V., S. E. Wert, K. H. Kaestner, and J. A. Whitsett. Stage-specific regulation of respiratory epithelial cell differentiation by Foxa1. *Am J Physiol Lung Cell Mol Physiol* 289: L750–L759, 2005; doi:10.1152/ajplung.00151.2005.—Foxa1 is a member of the winged helix family of transcription factors that is expressed in epithelial cells of the conducting airways and in alveolar type II cells of the lung. To determine the role of Foxa1 during lung morphogenesis, histology and gene expression were assessed in lungs from *Foxa1*$^{-/-}$ gene-targeted mice from embryonic day (E) 16.5 to postnatal day (PN) 13. Deletion of *Foxa1* perturbed maturation of the respiratory epithelium at precise times during lung morphogenesis. While dilatation of peripheral lung saccules was delayed in *Foxa1*$^{-/-}$ mice at E16.5, sacculation was unperturbed later in development (E17.5–E18.5). At PN5, alveolarization was markedly delayed in *Foxa1*$^{-/-}$ mice; however, by PN13 lung histology was comparable to wild-type controls. Clara cell secretory protein (CCSP), prosurfactant protein (SP)-C, and SP-B protein content and immunostaining were decreased in *Foxa1*$^{-/-}$ mice between E16.5 and E18.5 but normalized after birth. Timing and sites of expression of thyroid transcription factor-1, Foxj1, and β-tubulin were unaltered in lungs of *Foxa1*$^{-/-}$ mice. In vitro, Foxa1 regulated the activity of CCSP and SP-A, SP-B, SP-C, and SP-D promoters as assessed by luciferase reporter assays in HeLa, H441, and MLE15 cells. Although Foxa1 regulates respiratory epithelial differentiation and structural maturation of the lung at precise developmental periods, the delay in maturation is subsequently compensated at times to enable respiratory function and restore normal lung structure after birth.

lung; development; forkhead box family; transcription factor

FOXA1 IS A MEMBER of the winged helix family of transcription factors and shares structural similarities with Foxa2 and Foxa3 (previously termed HNF3α, HNF3β, and HNF3γ, respectively). *Foxa* genes are widely expressed during embryonic development in vertebrates. During formation of the definitive endoderm, Foxa2 is expressed before Foxa1 and Foxa3 (2, 29, 36). In the early embryo, Foxa2 is expressed in the node, notochord, and floor plate, whereas Foxa1 is detected only in the notochord and floor plate (2, 29, 34, 36). Later in embryonic development and adulthood, Foxa1 and Foxa2 are detected in tissues of endodermal, ectodermal, and mesodermal origins (3, 18, 21).

In the lung, Foxa1 and Foxa2 are first expressed at the onset of lung bud formation and are present in the adult lung, where they are coexpressed in epithelial cells of conducting airways and in type II epithelial cells in the alveoli (3). Foxa2 is strictly required during the alveolar period of lung morphogenesis as revealed by tissue-specific gene ablation (41, 42). Foxa2 plays an important role during alveolarization and regulates epithelial cell differentiation after birth. When Foxa2 is deleted in epithelial cells of the developing lung (*Foxa2*$^{\Delta/\Delta}$ mice), abnormalities in alveolarization are observed at PN3 that are associated with decreased alveolar septation and fewer peripheral lung saccules. At postnatal day (PN) 16 and thereafter, *Foxa2*$^{\Delta/\Delta}$ mice develop emphysema and goblet cell hyperplasia in the bronchi and bronchioles (41). Newborn mice lacking *Foxa2* in the lung develop severe pulmonary disease on the first day of life with the features of respiratory distress syndrome. Thus Foxa2 plays a critical role during the transition to air breathing at birth (42). *Foxa2* regulates the transcription of several genes that play important roles in lung morphogenesis and homeostasis, including *Titf1* (15), *Sftpb* (6), and *Scgblal* (4, 5). Although the sites of expression of Foxa1 and Foxa2 overlap in the developing and mature lung (3), the role of Foxa1 in lung development and function has not been established.

Targeted disruption of *Foxa1* in mice is characterized by reduced survival after birth due to severe hypoglycemia and dehydration (19, 39) and is associated with abnormally low glucagon levels. No changes were observed in expression of genes associated with glucose metabolism or in transcription factors that might compensate for the lack of Foxa1 in the liver (19). Despite growth retardation, no apparent morphological abnormalities were observed in tissues expressing Foxa1, including the gastrointestinal tract, liver, and pancreas. In this study, we assessed the role of Foxa1 during lung development. We demonstrate that Foxa1 regulated maturation of respiratory epithelial cells during the pre- and postnatal period.

MATERIALS AND METHODS

Animal husbandry. *Foxa1*$^{+/-}$ mice (129SvEv × C57BL/6) were derived at the University of Pennsylvania, as previously described (19), and were maintained as heterozygotes. Transgenic mice were identified by PCR with genomic DNA from the tails of fetal and postnatal mice, as previously described (32). Animals were housed in pathogen-free conditions according to protocols approved by Institutional Animal Care and Use Committee at Cincinnati Children's Hospital Research Foundation. All animals were housed in humidity- and temperature-controlled rooms on a 12:12-h light-dark cycle and were allowed food and water ad libitum. There was no serological evidence of either pulmonary or systemic pathogens in sentinel mice maintained within the colony. No serological evidence of viral infection or histological evidence of bacterial infection was detected in representative mice.

Tissue preparation and immunohistochemistry. The body and lung weight data were collected at the time of death. For embryonic data,

Address for reprint requests and other correspondence: J. A. Whitsett, Cincinnati Children's Hospital Medical Center, Divs. of Neonatology and Pulmonary Biology, 3333 Burnet Ave., Cincinnati, OH 45229-3039 (e-mail: jeff.whitsett@cchmc.org).

The costs of publication of this article were defrayed in part by the payment of page charges. The article must therefore be hereby marked "*advertisement*" in accordance with 18 U.S.C. Section 1734 solely to indicate this fact.

gestational age was determined by detection of the vaginal plug [as embryonic day (E) 0.5] and correlated with the length and weight of each pup at the time of death. Whole embryos were weighed after being removed from the yolk sac, washed, and dried. For the postnatal study, the mice were first weighed and then killed by an injection of 0.25 ml of anesthetic (ketamine, xylazine, acepromazine) and exsanguinated. In both cases, wet lung weights were measured after the heart, trachea, and bronchi have been removed. Embryonic lungs were immersed in 4% paraformaldehyde in PBS (20 mM Tris·HCl, pH 7.6, 137 mM NaCl), whereas postnatal lungs were inflation fixed with the same fixative at 25 cmH_2O before immersion. Lungs were fixed overnight, washed with PBS, dehydrated in a series of alcohols, and embedded in paraffin. Immunohistochemistry was performed on tissue sections by a microwave antigen-retrieval technique for the transcription factors (38). Sections were pretreated with 3% H_2O_2 in methanol for inactivation of endogenous peroxidase and then blocked in 4% normal goat serum for 2 h before incubation with the primary antibody overnight at 4°C. Antibodies used were generated to: prosurfactant protein (SP)-C (1:1,000, rabbit polyclonal, AB3428, Chemicon), Clara cell secretory protein (CCSP, 1:7,500, rabbit polyclonal; kindly provided by Dr Barry Stripp, University of Pittsburgh), SP-B (1:1,000 to 1:2,000, rabbit polyclonal, Chemicon, Temecula, CA), thyroid transcription factor (TTF-1, 1:1,000, rabbit polyclonal, generated in this laboratory), Foxa2 [1:8,000, rabbit polyclonal, (3)], Foxj1 [1:8,000, rabbit polyclonal (40)], and β-tubulin (1:800, mouse monoclonal; ONS1A6, BioGenex). After being rinsed, tissue sections were incubated with biotinylated goat anti-guinea pig IgG or goat anti-rabbit IgG (7.5 μg/ml; Vector Laboratories, Burlingame, CA) for 30 min and detected with an avidin-biotin peroxidase complex detection kit (Vectastain Elite ABC kit; Vector Laboratories, Burlingame, CA) using nickel-diaminobenzidine as a substrate. The precipitation reaction was enhanced with Tris-cobalt, and the sections were counterstained with 0.1% of nuclear fast red. All experiments shown are representative of findings from at least four independent dams, each generating at least one or two *Foxa1*$^{-/-}$ mice that were compared with *Foxa1*$^{+/+}$ littermates.

For ultrastructural analysis, lung tissue from E17.5 and E18.5 *Foxa1*$^{-/-}$ mice and littermate controls (matched for body weight) was fixed in modified Karnovsky's fixative, consisting of 2% glutaraldehyde and 2% paraformaldehyde in 0.1 M sodium cacodylate buffer (SCB) plus 0.1% calcium chloride (pH 7.3). The tissue was postfixed in 1% osmium tetroxide in 0.1 M SCB, dehydrated, and embedded in epoxy resin (EMbed 812; Electron Microscopy Sciences, Fort Washington, PA), as previously described (46). Ultrathin sections were viewed in a Hitachi H-7600 transmission electron microscope, and digitized images were collected with an AMT Advantage Plus 2K × 2K digital camera (Advanced Microscopy Techniques, Danvers, MA).

Morphometry. Morphometric measurements were performed on mice at PN5 and PN13. Three to five mice of both genotypes were studied at each age. The overall proportion (% fractional area) of respiratory parenchyma and air space was determined by a point-counting method (7, 43). Measurements were performed on two sections taken at intervals throughout the left, right upper, or right lower lobes. Slides were viewed by through a ×20 objective, and the images (fields) were transferred by video camera to a computer screen using Metamorph imaging software (Universal Imaging, West Chester, PA). A computer-generated, 121-point lattice grid was superimposed on each field, and the number of intersections (points) falling over respiratory parenchyma (alveoli and alveolar ducts) or air space was counted. Points falling over bronchioles, large vessels, and smaller arterioles and venules were excluded from the study. Fractional areas (% Fx area) were calculated by dividing the number of points for each compartment (n) by the total number of points contained within the field (N), and then multiplying by 100: % Fx area = $n/N \times 100$. Fifteen fields per section were analyzed to gather the data. The x- and y-coordinates for each field measured were selected by a random number generator. Likewise, counting of secondary septa was performed on five fields per section of three to five mice of both genotypes and results were normalized per lung area.

RNA analysis. S1 nuclease protection and RNase protection assays were performed as described previously (16, 33). mRNAs encoding SP-A, SP-B, SP-C, SP-D, CCSP, TTF-1, and Foxa2 were quantified by either S1 nuclease protection assay or RNase protection assay with ribosomal protein L32 as an internal control. A rat Foxa2 probe was kindly provided by Dr. R. Costa of the University of Illinois. Figures are representative of at least four individual mice at each time for each group.

Cell culture and transfection assays. Mouse lung epithelial cells, MLE-15, an immortalized mouse lung epithelial cell line that maintains some morphological and functional characteristics of type II epithelial cells, were cultured in HITES medium (45). Lung adenocarcinoma cells NCI-H441 (ATCC HTB 174) and cervical cancer cells HeLa (ATCC CCl-2) were obtained from the American Type Culture Collection (ATCC, Rockville, MD). HeLa cells were grown in Dulbecco's modified Eagle's medium, and H441 cells were grown in RPMI containing 4.5g/l D-glucose and 10 mM HEPES, both media supplemented with 50 units of penicillin/ml, 50 μg of streptomycin/ml, and 10% fetal calf serum. Cells were transfected with the Effectene transfection reagent (Qiagen) according to the manufacturer's protocol. The reporter constructs were: 1.1 kb mouse SP-A-luc, 0.5 kb human SP-B-luc, 1.8 kb mouse SP-B-luc, 4.8 kb mouse SP-C-luc, 0.7 kb mouse SP-D-luc (12), 2.3 kb rCCSP-luc, or 3.7 kb mouse MUC5AC-luc (kindly provided by Dr. Carol Basbaum, University of San Francisco) (22) and were cotransfected with either empty vector pcDNA3.1 or pcDNA3.1 containing the full-length mouse Foxa1 cDNA. Forty-eight hours after transfection, luciferase activity was assessed and normalized for cotransfection efficiency by β-galactosidase activity. All transfections were performed in triplicate. pcDNA3.1 (Invitrogen) and pCMV β-galactosidase (Clontech) vectors were used to normalize DNA and transfection efficiency, respectively.

Statistical analysis. ANOVA and Student's t-test were used to determine differences between groups. In the morphometric study, statistical differences were determined by the χ^2-test for fractional areas and unpaired Student's t-test for comparison of septa formation. Values for all measurements were expressed as means ± SE, and P values for significance were <0.05.

RESULTS

Lung morphogenesis is temporarily delayed in Foxa1-deficient mice. To assess the role of Foxa1 in lung development, we used *Foxa1*$^{-/-}$ gene-targeted mice (19). Embryos obtained before birth showed no apparent morphological abnormalities. As reported previously, most of the *Foxa1*$^{-/-}$ mice died within the first week of life. The longest survivors died at PN13. Body weights in *Foxa1*$^{-/-}$ and *Foxa1*$^{+/+}$ control littermates were not altered before birth (Fig. 1*A*). However, at PN5, the *Foxa1*$^{-/-}$ mice had a lower body weight compared with littermates. In contrast, the *Foxa1*$^{+/+}$ and *Foxa1*$^{+/-}$ mice gained weight normally. The lung-to-body weight (LW/BW) ratios were similar in each genotype at all time points examined, indicating that lung growth was not selectively altered in *Foxa1*$^{-/-}$ mice (Fig. 1*C*) but corresponded to general body growth.

Next we investigated perinatal lung development in embryos at E16.5, E17.5, and E18.5 and pups at PN5 and PN13. At E16.5, morphological maturation of the lungs was delayed in *Foxa1*$^{-/-}$ mice compared with control littermates (Fig. 2, *A* and *B*). Whereas lung maturation had reached the saccular stage of lung development, with dilatation of the distal lung saccules occurring in *Foxa1*$^{+/+}$ mice, lung morphology in the

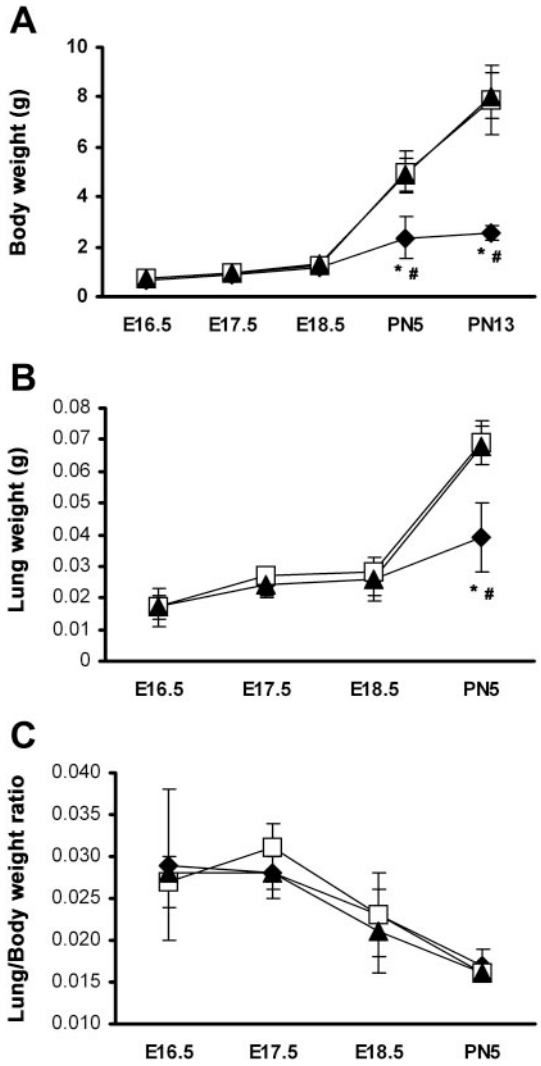

Fig. 1. Deletion of Foxa1 inhibits postnatal but not prenatal somatic growth. Body weight (*A*), lung weight (*B*), and lung-to-body weight ratios (*C*) of Foxa1$^{-/-}$ (◆), Foxa1$^{+/-}$ (□), and Foxa1$^{+/+}$ (▲) mice was measured from embryos harvested at embryonic day (E) 16.5, E17.5, and E18.5, and pups at postnatal day (PN) 5 and PN13. Values are means ± SE. *$P < 0.001$ for +/+ vs. −/−; #$P < 0.001$ for +/− vs. −/−.

Foxa1$^{-/-}$ mice remained in the canalicular stage. However, by E17.5 and E18.5, lungs from *Foxa1*$^{-/-}$ and *Foxa1*$^{+/+}$ mice were similar with no obvious structural differences in saccule formation (Fig. 2, *C–F*). After birth, differences between the lungs of *Foxa1*$^{-/-}$ mice and control littermates were readily apparent (Fig. 2, *G* and *H*). At PN5, lungs from *Foxa1*$^{-/-}$ mice had thinner inter-air space septa, larger and fewer air spaces, and a reduction in the number of secondary septa compared with the *Foxa1*$^{+/+}$ mice. By PN13, septation had progressed to normal in the surviving *Foxa1*$^{-/-}$ mice (Fig. 2, *I* and *J*). Morphometric analysis showed significant statistical differences in the relative proportion of air space (Fig. 3*A*) and respiratory parenchyma (Fig. 3*B*) at PN5 in the *Foxa1*$^{-/-}$ mice compared with the *Foxa1*$^{+/+}$ mice. The percentage of fractional area of air space was increased significantly ($P < 0.001$) in *Foxa1*$^{-/-}$ mice, whereas no statistical difference was observed at PN13 between the two groups. Likewise, respiratory parenchyma was decreased at PN5 in the *Foxa1*$^{-/-}$ mice compared with the *Foxa1*$^{+/+}$ mice, whereas no statistical difference was noticed at PN13. Study of alveolar septation shows that secondary septa formation is dramatically reduced in the *Foxa1*$^{-/-}$ mice compared with the *Foxa1*$^{+/+}$ mice at PN5. The morphometric results were consistent with the histological findings.

At the ultrastructural level, at E17.5, ciliated and nonciliated columnar epithelial cells were present in conducting airways of *Foxa1*$^{-/-}$ and *Foxa1*$^{+/+}$ mice. Cuboidal type II cells were observed throughout the peripheral lung epithelium in both genotypes. Type II cells in the *Foxa1*$^{-/-}$ mice had more glycogen, fewer lamellar bodies, and less secreted surfactant

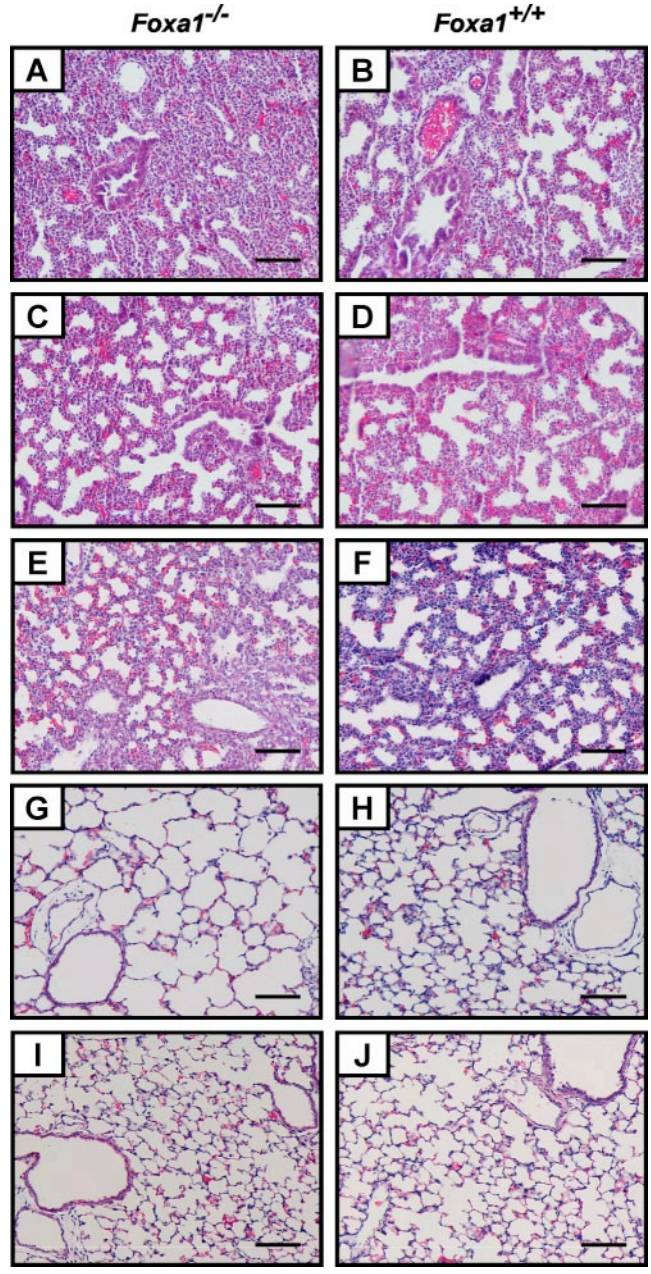

Fig. 2. *Foxa1* deletion perturbs lung morphogenesis. Lung sections of *Foxa1*$^{-/-}$ (*A, C, E, G, I*) and *Foxa1*$^{+/+}$ mice (*B, D, F, H, J*) were prepared on E16.5 (*A, B*), E17.5 (*C, D*), E18.5 (*E, F*), PN5 (*G, H*), and PN13 (*I, J*) and stained with hematoxylin and eosin to assess lung morphology. Figure is representative of at least 4 individual mice at each time. Scale bar: 500 μm.

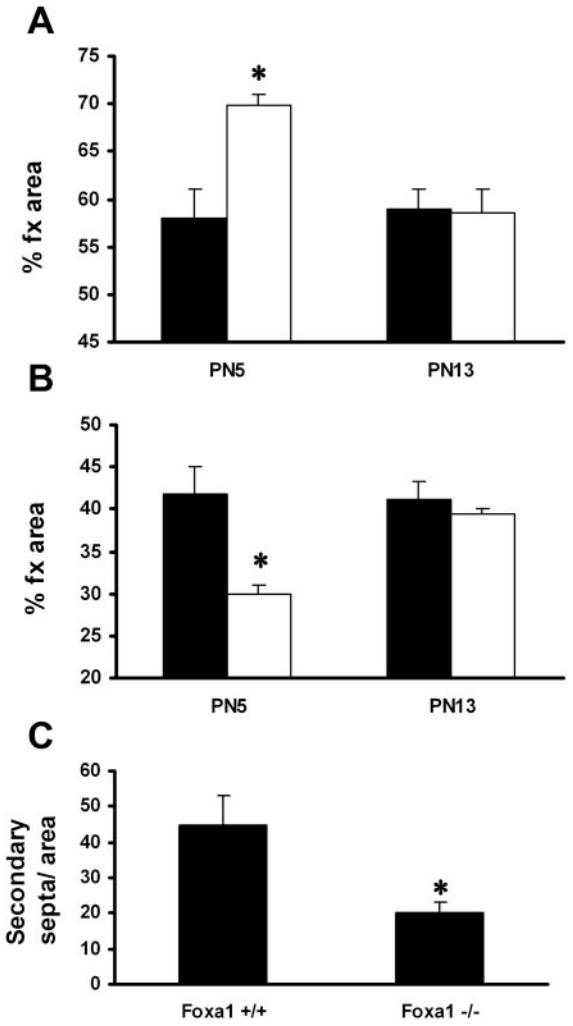

Fig. 3. Morphometric analysis during alveolarization. Changes in fractional areas (% fx area) of air space (*A*) and respiratory parenchyma (*B*) were determined at PN5 and PN13 in *Foxa1*$^{-/-}$ (open bar) and *Foxa1*$^{+/+}$ mice (solid bar). Data are expressed as % fx area and represent means ± SE (*$P <$ 0.001 for +/+ vs. −/−). Formation of secondary septa (*C*) was estimated at PN5 in *Foxa1*$^{-/-}$ and *Foxa1*$^{+/+}$ mice. Data are expressed as the number of secondary septa per lung area and represent means ± SE (*$P < 0.001$ for +/+ vs. −/−).

compared with the *Foxa1*$^{+/+}$ mice control littermates (Fig. 4). Squamous type I cells were infrequent in the *Foxa1*$^{-/-}$ mice. At E18.5, no differences were observed at the ultrastructural level in the conducting airways or peripheral epithelium between the *Foxa1*$^{-/-}$ and *Foxa1*$^{+/+}$ mice (data not shown).

Effects of Foxa1 deletion on epithelial cell gene expression. To evaluate the differentiation of respiratory epithelial cells in *Foxa1*$^{-/-}$ mice, we performed immunohistochemistry for differentiation-dependent markers that were specific for conducting or peripheral airways from E16.5 to PN13. CCSP, a marker for nonciliated bronchiolar cells, was absent in the conducting airways of *Foxa1*$^{-/-}$ mice at E16.5 and E17.5 and was readily detected, albeit at relatively reduced levels, at E18.5. In *Foxa1*$^{+/+}$ mice, CCSP was detected at E16.5 (Fig. 5). However, after birth, no differences in CCSP staining were observed in *Foxa1*$^{-/-}$ and *Foxa1*$^{+/+}$ mice. Expression of pro- and mature SP-B, a surfactant protein expressed by both type II and bronchiolar cells, was decreased in the *Foxa1*$^{-/-}$ mice at E16.5, E17.5, and E18.5 (Fig. 6, *A–F*). After birth, intensity of SP-B staining was decreased in the *Foxa1*$^{-/-}$ mice at PN5, whereas no differences were observed at PN13 (Fig. 6, *G–J*). Likewise, intensity of staining for pro-SP-C, a selective marker for type II cells, was decreased in the *Foxa1*$^{-/-}$ mice at E16.5–E18.5 (Fig. 7, *A–F*). Again after birth, staining for pro-SP-C was similar the *Foxa1*$^{-/-}$ mice and control littermates (Fig. 7, *G–I*). T1α (a type I cell marker), Foxj1, and β-tubulin (ciliated cell markers) were also unaltered after birth. Consistent with these observations, immunoblotting studies demonstrated that the abundance of SP-B and CCSP was decreased at E18.8 and PN5 in *Foxa1*$^{-/-}$ mice (data not shown). In contrast, the abundance of SP-A and SP-D in lung homogenates was not altered in *Foxa1*$^{-/-}$ mice compared with wild-type controls at any of the time points.

To determine whether the changes in SP-B, SP-C, and CCSP immunostaining were associated with changes in their respective mRNAs, we performed S1 nuclease assays on lung RNA samples from *Foxa1*$^{-/-}$ and *Foxa1*$^{+/+}$ mice at E16.5, E17.5, E18.5, and PN5 (Fig. 8). SP-A mRNA levels were decreased in *Foxa1*$^{-/-}$ mice at PN5 (Fig. 8*A*). At E16.5, SP-B and SP-C mRNAs were significantly reduced in the *Foxa1*$^{-/-}$ mice compared with the control littermates. In contrast, at E17.5 and later, no differences in SP-B, SP-C, and SP-D mRNAs were observed in the *Foxa1*$^{-/-}$ mice (Fig. 8*D*). Consistent with

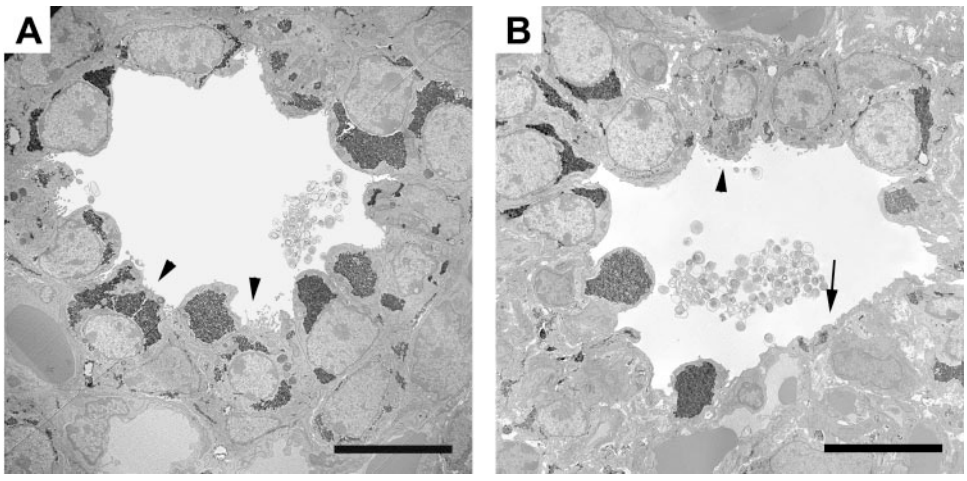

Fig. 4. Lung ultrastructure of E17.5 *Foxa1*$^{-/-}$ and *Foxa1*$^{+/+}$ mice. Electron microscopy was performed on lungs from *Foxa1*$^{-/-}$ (*A*) and *Foxa1*$^{+/+}$ (*B*) mice at E17.5. Cuboidal type II cells (arrowhead) with apical microvilli were observed in both *Foxa1*$^{-/-}$ and *Foxa1*$^{+/+}$ mice. Organized glycogen was increased in type II cells of *Foxa1*$^{-/-}$ mice. Lamellar bodies and secreted surfactant were less abundant in the *Foxa1*$^{-/-}$ compared with the *Foxa1*$^{+/+}$ mice. Squamous type I cells (arrow) were frequently observed in the *Foxa1*$^{+/+}$ mice compared with the *Foxa1*$^{-/-}$ mice. Scale bar: 10 μm.

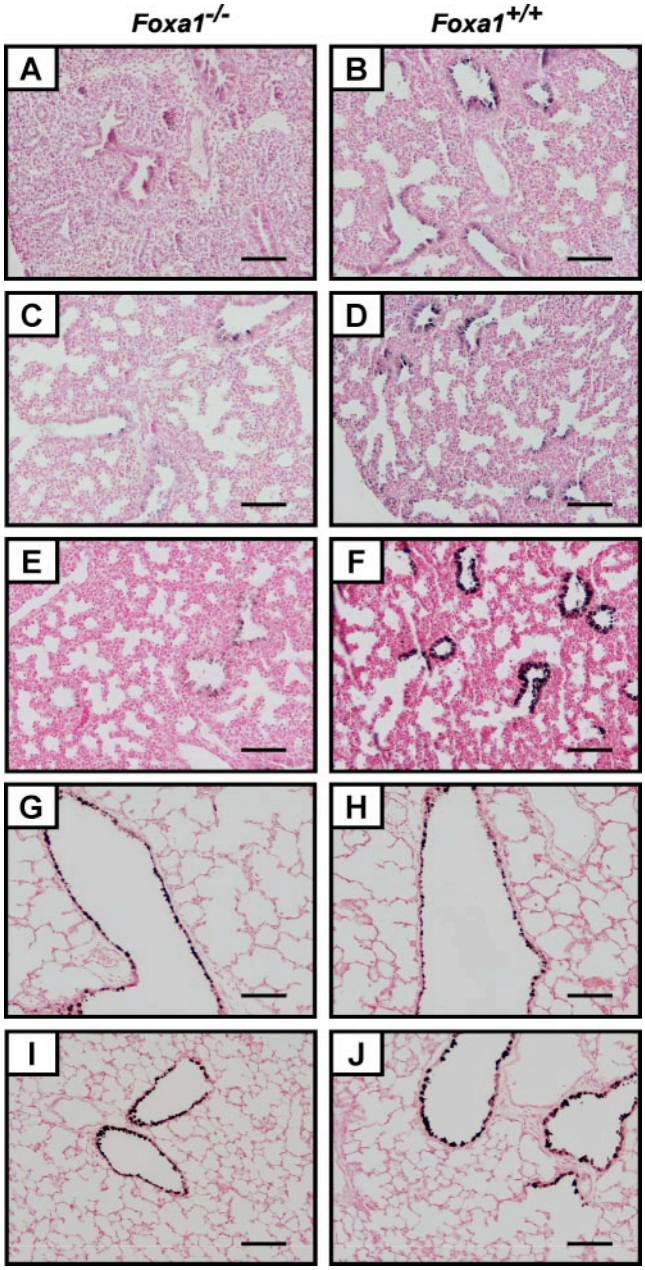

Fig. 5. Delay of Clara cell secretory protein (CCSP) expression in *Foxa1*$^{-/-}$ mice. Lung sections of *Foxa1*$^{-/-}$ mice (*A, C, E, G, I*) and *Foxa1*$^{+/+}$ mice (*B, D, F, H, J*) were prepared on E16.5 (*A, B*), E17.5 (*C, D*), E18.5 (*E, F*), PN5 (*G, H*), and PN13 (*I, J*) and stained for CCSP. Figure is representative of at least 4 individual mice at each time. Scale bar: 500 μm.

decreased immunostaining, expression of CCSP mRNA was markedly reduced in *Foxa1*$^{-/-}$ mice from E16.5 to birth (Fig. 8*E*). CCSP mRNA was decreased by 50% at E17.5 and E18.5. After birth, CCSP mRNA was similar in *Foxa1*$^{-/-}$ and *Foxa1*$^{+/+}$ mice. Thus maturation of both lung morphology and expression of epithelial differentiation were delayed in late gestation in *Foxa1*$^{-/-}$ mice.

Foxa1 regulates lung epithelial cell gene expression in vitro. To assess whether Foxa1 directly regulated lung epithelial cell gene expression, we cotransfected luciferase reporter constructs driven by SP-A, SP-B, SP-C, SP-D, and CCSP promoters with increasing concentrations of a Foxa1 expression vector into HeLa, H441, or MLE-15 cells. Foxa1 significantly increased the activity of the SP-A, SP-D, and CCSP-luciferase constructs in a dose-dependent manner (Fig. 9, *A, E,* and *F*). In contrast, Foxa1 inhibited the murine SP-C promoter construct (Fig. 9*D*). Foxa1 inhibited both human and mouse SP-B promoter activity in H441 and MLE-15 cells (Fig. 9, *B* and *C*). Foxa1 did not alter activity of the MUC5AC-luciferase construct (data not shown). Thus Foxa1 activates a number of lung epithelium-specific genes including SP-A, SP-D, and CCSP in vitro. While Foxa1 and Foxa2 bind to the same DNA binding motifs, transcriptional effects of Foxa1 are both similar (42) and distinct (13, 37, 41) from Foxa2 on various target genes.

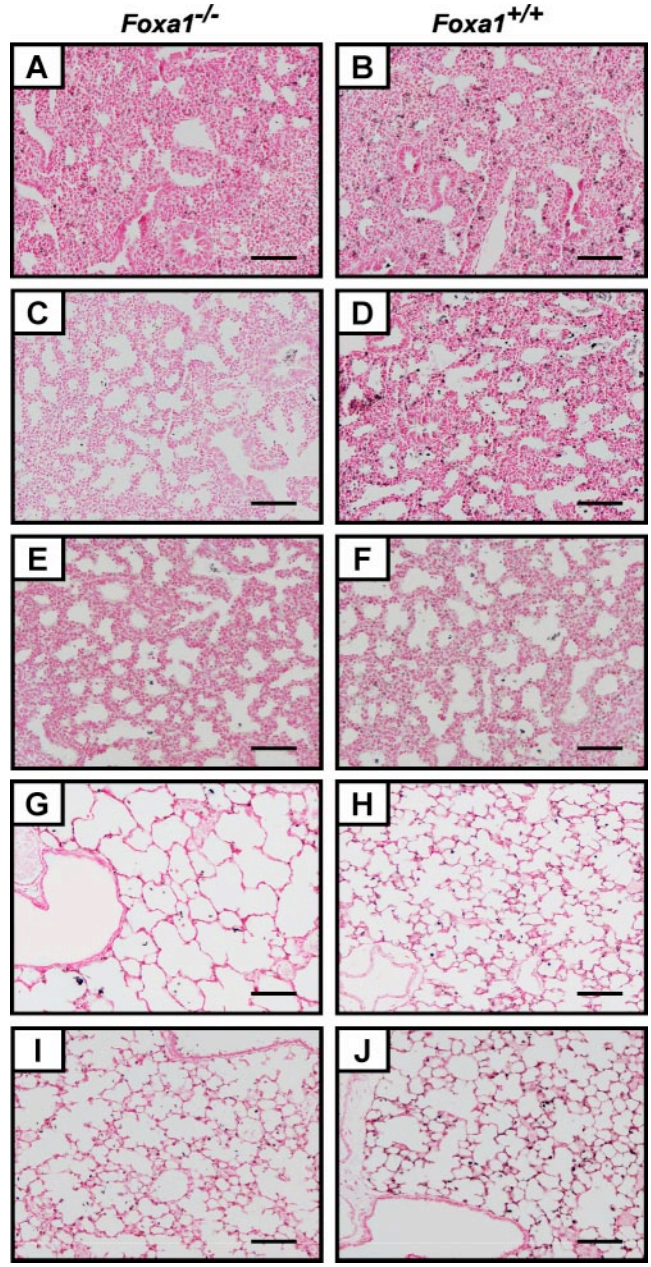

Fig. 6. Stage-specific decrease in SP-B in *Foxa1*$^{-/-}$ mice. Lung sections of *Foxa1*$^{-/-}$ mice (*A, C, E, G, I*) and *Foxa1*$^{+/+}$ mice (*B, D, F, H, J*) were prepared on E16.5 (*A, B*), E17.5 (*C, D*), E18.5 (*E, F*), PN5 (G, H), and PN13 (*I, J*) and stained to assess SP-B expression. Figure is representative of at least 4 individual mice at each time. Scale bar: 500 μm.

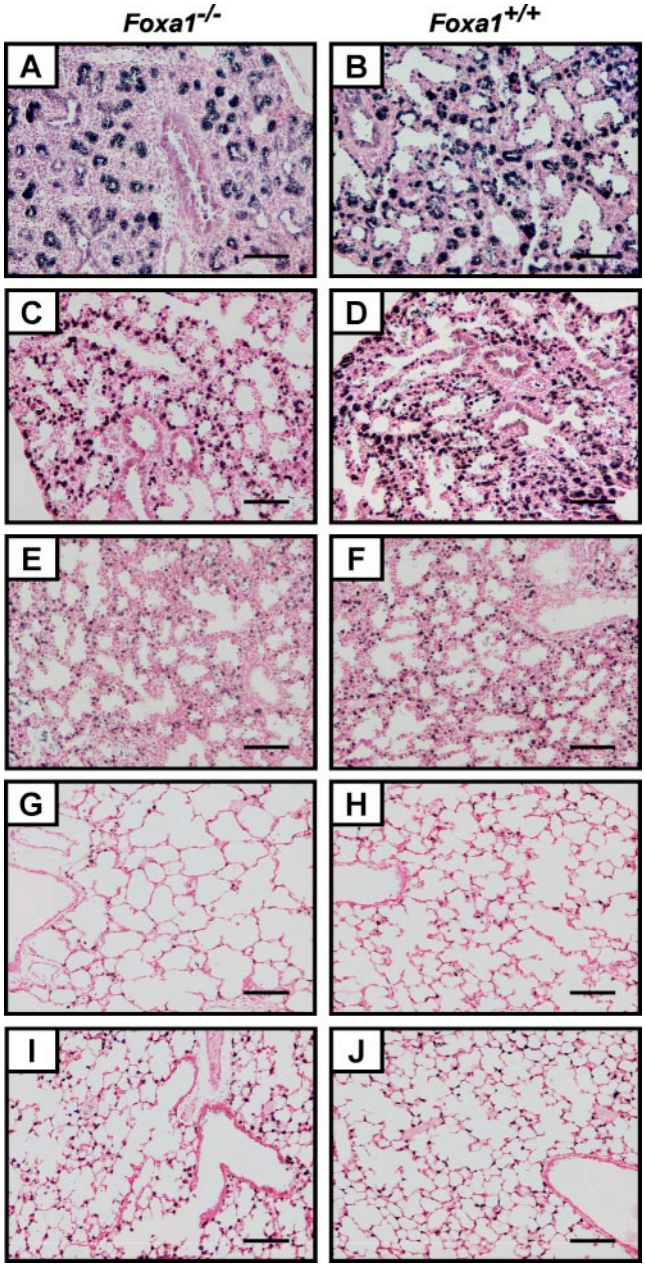

Fig. 7. Stage-specific decrease in prosurfactant protein (SP)-C in *Foxa1*$^{-/-}$ mice. Lung sections of *Foxa1*$^{-/-}$ mice (*A, C, E, G, I*) and *Foxa1*$^{+/+}$ mice (*B, D, F, H, J*) were prepared on E16.5 (*A, B*), E17.5 (*C, D*), E18.5 (*E, F*), PN5 (*G, H*), and PN13 (*I, J*) and stained to assess pro-SP-C expression. Figure is representative of at least 4 individual mice at each time. Scale bar: 500 μm.

The discrepancies between in vitro and in vivo effects of Foxa1 on various target genes suggests that Foxa1 likely to have both direct and indirect effects on gene transcription in the developing lung. Alternatively, compensatory mechanisms may further influence gene expression at various times in development.

Transcription factors expression in Foxa1$^{-/-}$ *mice.* To determine whether other transcription factors could compensate for the lack of Foxa1 in the regulation of lung epithelial cell genes, we assessed the expression of Foxa2 and TTF-1, markers for both proximal and distal airways, by immunohistochemistry. Sites and intensity of Foxa2 and TTF-1 staining were similar in both *Foxa1*$^{-/-}$ and *Foxa1*$^{+/+}$ mice in bronchiolar and alveolar epithelial cells at all development stages examined (Fig. 10 and data not shown). Consistent with these observations, no differences in Foxa2 or TTF-1 mRNA levels were observed in *Foxa1*$^{-/-}$ mice at various time points (Fig. 11).

DISCUSSION

Although Foxa1 is not required for respiration at birth, deletion of Foxa1 influences lung morphogenesis and epithelial cell differentiation at distinct times during perinatal development. Because delayed lung maturation may impair respiratory

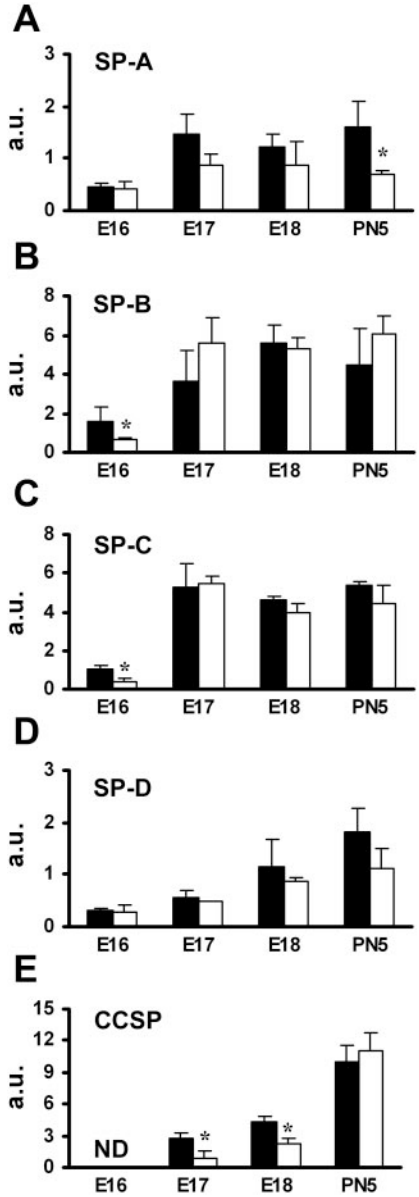

Fig. 8. S1 nuclease assay for surfactant protein and CCSP mRNAs. S1 nuclease assays were used to quantitate SP-A, SP-B, SP-C, SP-D, and CCSP mRNAs in lungs from *Foxa1*$^{-/-}$ (□) and *Foxa1*$^{+/+}$ (■) mice at E16.5, E17.5, E18.5, and PN5 and compared with L32 mRNA. Histograms show a quantitative representation of SP-A (*A*), SP-B (*B*), SP-C (*C*), SP-D (*D*), and CCSP (*E*) mean mRNA values from *Foxa1*$^{-/-}$ and *Foxa1*$^{+/+}$ mice. Results were expressed in arbitrary units (a. u.). *$P < 0.05$ for +/+ vs. −/−. ND, not detected.

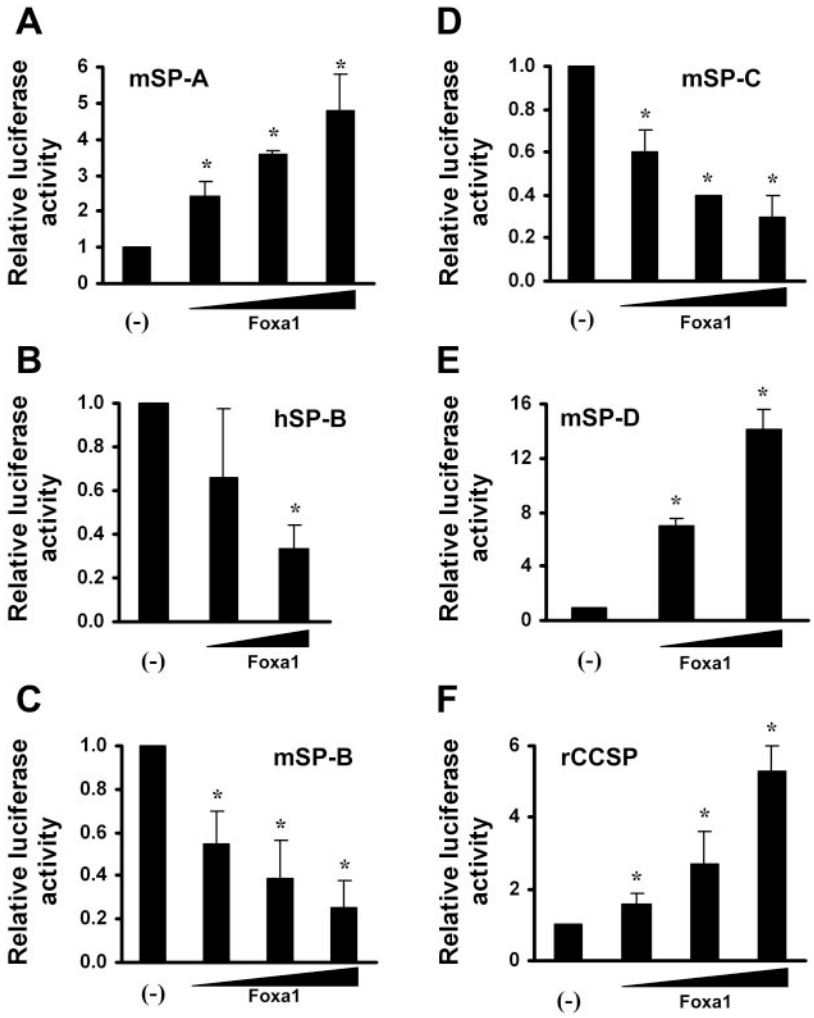

Fig. 9. Foxa1 regulates surfactant protein and CCSP promoters in vitro. Effect of Foxa1 on promoter activity was assessed after cotransfection of a fixed amount of the following: SP-A-Luc (0.5 μg) with increasing amounts of Foxa1 expression plasmid (pcDNA3.1-Foxa1) at 0 (−), 0.5, 1.0, and 2 μg per well into HeLa cells (*A*); human (h) SP-B-Luc (0.5 μg) with 0 (−), 1.0, and 2 μg per well into H441 cells (*B*); murine (m) SP-B-Luc (0.5 μg) with 0 (−), 0.5, 1.0, and 2 μg per well into H441 cells (*C*); mSP-C-Luc (0.5 μg) with 0 (−), 0.5, 1.0, and 2 μg per well into MLE15 cells (*D*); mSP-D-Luc (0.5 μg) with 0 (−), 2, and 4 μg per well into MLE15 cells (*E*); and rat (r) CCSP-Luc (0.5 μg) with 0 (−), 0.5, 1.0, and 2 μg per well into HeLa cells (*F*). Results are expressed as the means ± SE of 3 experiments performed in triplicate. *$P < 0.05$ vs. (−) condition.

function during the transition to air breathing in neonates, Foxa1 may play important roles in stage-specific functions of the lung and may influence neonatal adaptation in preterm infants who have susceptibility to respiratory distress syndrome. Foxa1 and Foxa2 are coexpressed in epithelial cells lining tubules during lung morphogenesis and in both conducting airways and alveoli in the adult lung. Both Foxa1 and Foxa2 influence the expression of a number of genes that are dynamically regulated in epithelial cells of the developing lung. The present study demonstrates that the deletion of Foxa1 perturbs maturation of the respiratory epithelium at precise times during lung morphogenesis. Foxa1 delayed the onset of sacculation and expression of differentiated epithelial cell markers before birth. Likewise, deletion of Foxa2 perturbed alveolarization in the early postnatal period.

Foxa transcription factors regulate cell differentiation in various organs such as liver, pancreas, lung, and brain. Before birth, a delay in structural maturation and expression of both proximal and peripheral epithelial cell markers of the lung was observed in the *Foxa1*$^{-/-}$ mice. During the antenatal period, body weight as well as LW/BW ratios were similar in *Foxa1*$^{-/-}$ mice, indicating that Foxa1 was not required for normal fetal growth, in accordance to previous findings (17). *Foxa1*$^{-/-}$ mice did not gain weight after PN3 despite evidence of suckling. LW/BW ratio in *Foxa1*$^{-/-}$ mice was similar to that in *Foxa1*$^{+/+}$ mice. Previous studies showed that caloric restriction causes a delay in lung morphogenesis, with more prominent effects observed during phases of growth and differentiation (23, 30, 35). Although surfactant phospholipid content was reduced, surfactant composition was normal in lungs of calorie-deprived animals before birth or during adulthood (8, 23). Thus *Foxa1* deletion delayed lung maturation independently of fetal growth.

Deletion of Foxa1 causes stage-specific delay in lung maturation. Before birth, *Foxa1* deletion in the mouse lung delayed maturation of alveolar type II cells and bronchiolar Clara cells. Immunostaining for SP-B and SP-C was detected in the *Foxa1*$^{-/-}$ mice but was reduced, whereas CCSP staining and mRNA were markedly delayed in the *Foxa1*$^{-/-}$ mice before birth. A discrepancy between mRNA levels and protein expression was observed for SP-B and SP-C. These results suggested that posttranscriptional mechanisms also influence surfactant protein expression and function. Lower SP-B and SP-C protein levels may be influenced by alterations in processing, routing, storage, secretion, and reuptake and are therefore not entirely dependant on transcriptional effects of Foxa1. Despite stage-specific decreases in SP-B and SP-C, *Foxa1*$^{-/-}$ mice survived at birth. It is possible that the delay in matura-

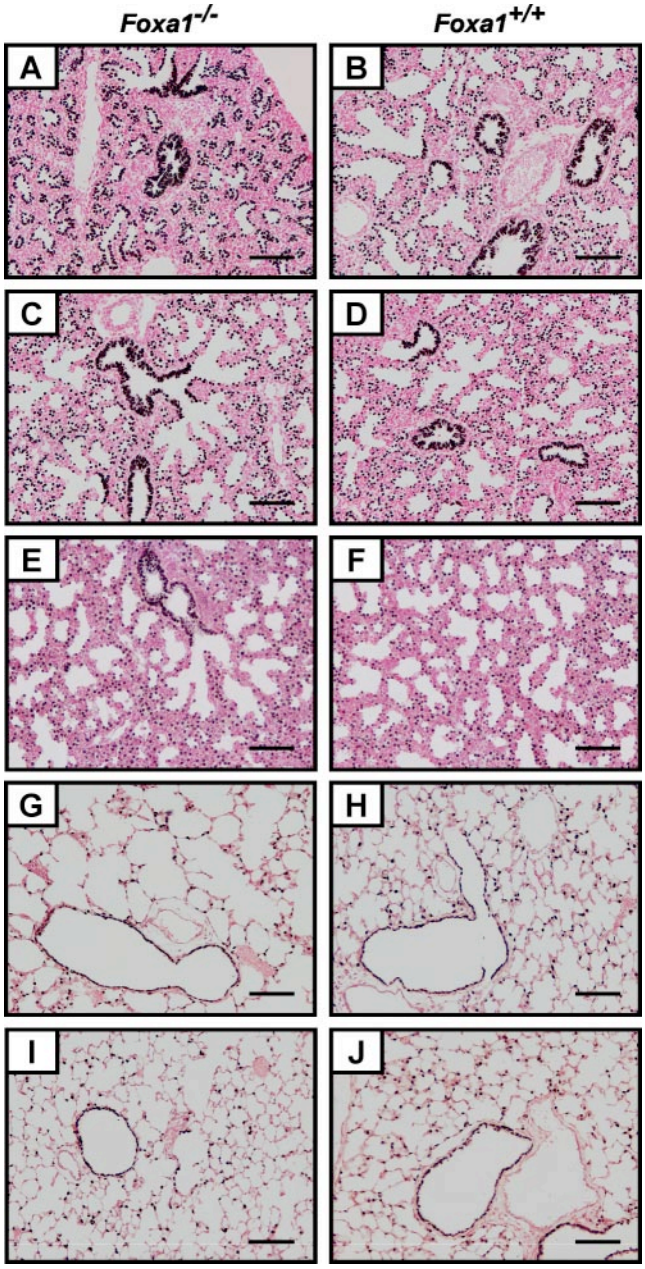

Fig. 10. Foxa2 expression in *Foxa1*$^{-/-}$ mice. Lung sections of *Foxa1*$^{-/-}$ mice (*A, C, E, G, I*) and *Foxa1*$^{+/+}$ mice (*B, D, F, H, J*) were prepared on E16.5 (*A, B*), E17.5 (*C, D*), E18.5 (*E, F*), PN5 (*G, H*), and PN13 (*I, J*) and stained for Foxa2. Figure is representative of at least 4 individual mice at each time. Scale bar: 500 μm.

tion before birth would render *Foxa1*-deficient mice susceptible to respiratory distress at earlier gestations.

Foxa1 deletion impairs the timing of perinatal alveolarization. In the mouse, alveolarization occurs in the postnatal period (PN4–PN21). In *Foxa1*$^{-/-}$ mice alveolarization was dramatically reduced at PN5 with a delay in formation of the secondary septa. However, expression of surfactant proteins and CCSP was identical in *Foxa1*$^{-/-}$ mice compared with wild-type controls at PN5. Despite a delay in alveolar septation, respiratory function was maintained in the *Foxa1*$^{-/-}$ mice. Increased serum cortisol was observed in *Foxa1*$^{-/-}$ compared with the *Foxa1*$^{+/+}$ mice (19, 39). Antenatal glucocorticoids accelerate maturation of the lung, thinning alveolar walls (24), and induce the expression of various markers of epithelial cell differentiation, including CCSP, SP-A, SP-B, and SP-C (31). In neonatal rats, glucocorticoids inhibit alveolarization, resulting in fewer and larger alveoli in the mature lung (25). Although alveolarization was perturbed in *Foxa1*$^{-/-}$ mice, alveolarization had nearly normalized by PN13, indicating *Foxa1* deletion did not permanently impair septation. In contrast, glucocorticoid exposure caused prolonged abnormalities in alveolar structure in rats (25). Whether changes in systemic glucocorticoids represent a compensatory mechanism by which lung maturation in *Foxa1*$^{-/-}$ mice is restored remains to be clarified.

Lung structure and gene expression, although impaired at precise times in *Foxa1*$^{-/-}$ mice, were restored at critical times in development, allowing breathing at birth and alveolarization postnatally. At E18.5, lung morphology and expression levels of SP-A, SP-B, SP-C, and SP-D, but not CCSP, were similar in *Foxa1*$^{-/-}$ and *Foxa1*$^{+/+}$ mice, indicating that an acceleration in lung maturation had occurred in the mutant mice. At PN13, alveolarization had improved markedly, indicating that acceleration of lung maturation had occurred in *Foxa1*$^{-/-}$ mice. We hypothesize that strong compensatory pathways correct the delay in lung maturation in *Foxa1*$^{-/-}$ mice, enabling respiratory function at birth and alveolarization during the postnatal period. Septation had improved by PN13 despite the growth retardation related to metabolic abnormalities in *Foxa1*$^{-/-}$ mice. Thus alveolar function and structure were maintained despite caloric deprivation and high levels of serum cortisol (25, 26).

The stage-specific recovery of maturation in lungs of the *Foxa1*$^{-/-}$ mice provides evidence that Foxa2 and/or other transcription factors are able to compensate for the lack of Foxa1. Foxa1 and Foxa2 share a highly conserved DNA binding motif and may compete for certain targets and, hence, may have both complementary and distinct functions at specific transcriptional targets (11, 17). Foxa1 mRNA was in-

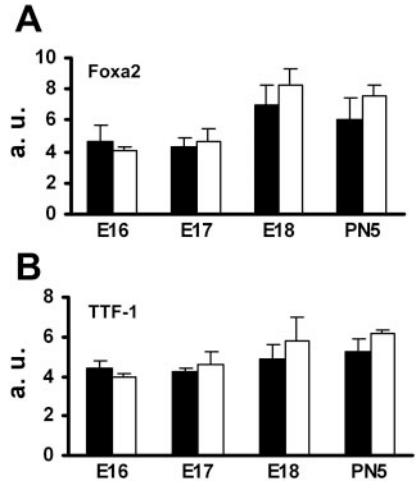

Fig. 11. RNA protection assay for estimation of Foxa2 and thyroid transcription factor (TTF)-1 mRNAs. RNA protection assays were used to quantitate Foxa2 and TTF-1 mRNAs in lungs from *Foxa1*$^{-/-}$ (□) and *Foxa1*$^{+/+}$ (■) mice at E16.5, E17.5, E18.5, and PN5 and compared with L32 mRNA. Histograms show a quantitative representation of Foxa2 (*A*) and TTF-1 (*B*) mean mRNA values from *Foxa1*$^{-/-}$ and *Foxa1*$^{+/+}$ mice. Results were expressed in a. u.

creased after deletion of Foxa2 in respiratory epithelial cells (42). In a recent study, Wan et al. (40) showed a 1.5-fold increase in Foxa2 mRNA in a microarray analysis of E18.5 *Foxa1*$^{-/-}$ lungs. In the present work, Foxa2 mRNA levels and staining were similar in *Foxa1*$^{+/+}$ and *Foxa1*$^{-/-}$ lungs. These results are supported by previous work of Kaestner et al. (19), showing that expression of Foxa2 and Foxa3 was not induced by the lack of Foxa1 in the liver.

Shared and distinct functions of Foxa1 and Foxa2. Foxa1 and Foxa2 regulate transcription of a number of genes expressed in the respiratory epithelium in vitro, including *Sftpb* and *Scgblal* (5, 6, 10, 37). In the present study, Foxa1 transactivated the mouse SP-A promoter in HeLa cells. A putative Foxa binding site was described by Alcorn et al. (1) on the SP-A promoter. In the *Foxa2*$^{\Delta/\Delta}$ mice, SP-A mRNA was significantly reduced, suggesting that Foxa2 regulates the SP-A promoter (41). It is surprising that Foxa1 inhibited the SP-C promoter in MLE-15 cells. These results are supported by previous findings demonstrating that Foxa1 did not activate an SP-C/CAT expression construct in MLE-15 cells (20). In the present study and that by Wan et al. (41), no changes were observed in SP-C expression in the *Foxa1*$^{-/-}$ and the *Foxa2*$^{\Delta/\Delta}$ mice. However, mice lacking both Foxa1 and Foxa2 in the respiratory epithelium completely lacked SP-C expression, demonstrating that a Foxa family member is required, either directly or indirectly, for expression of SP-C. As previously described (37), the rat CCSP promoter was activated by Foxa1 in HeLa cells in vitro. In the *Foxa1*$^{-/-}$ mice, CCSP mRNA content and immunostaining were markedly reduced before birth, suggesting that Foxa1 plays a critical role in the perinatal regulation of CCSP. However, after birth, CCSP expression was similar in the *Foxa1*$^{-/-}$ and *Foxa1*$^{+/+}$ mice, again indicating that compensatory mechanisms restored CCSP expression. In the present study, Foxa1 activated the mouse SP-D promoter, consistent with previous studies using the human SP-D promoter (14). Surprisingly, SP-B promoters were inhibited by cotransfection of Foxa1 cDNA in MLE-15 cells and H441 cells. Because Foxa1 plays dual roles in gene regulation by enhancing gene transcription and by acting on chromatin remodeling (9, 27), differences in activities of Foxa1 on the SP-B promoter may be cell type specific or influenced by developmental processes (6, 10). Because *Foxa1*$^{-/-}$ mice survived perinatally despite decreased SP-B staining, SP-B concentrations were adequate for respiratory function. Absence or severe reduction of SP-B in the fetal or adult lung is sufficient to cause respiratory failure (28, 44).

Deletion of Foxa1 caused specific delays in gene expression and structural maturation of the lung. Such stage-specific delay in maturation may influence perinatal adaptation in preterm and term neonates. Because Foxa1 regulates a number of genes critical for pulmonary homeostasis, abnormalities in the structure, function, or regulation of Foxa1 may render individuals susceptible to lung injury or disease after birth.

ACKNOWLEDGMENTS

The authors acknowledge technical contribution from Kara Von Zychlin, Georgianne Ciraolo for electron microscopy sectioning, and Vrushrank Davé.

GRANTS

This work was supported by National Institutes of Health Grants HL-61646 (J. A. Whitsett, S. E. Wert), HL-53687 (J. A. Whitsett, S. E. Wert), and DK-49210 (K. H. Kaestner).

REFERENCES

1. **Alcorn JL, Gao E, Chen Q, Smith ME, Gerard RD, and Mendelson CR.** Genomic elements involved in transcriptional regulation of the rabbit surfactant protein-A gene. *Mol Endocrinol* 7: 1072–1085, 1993.
2. **Ang SL, Wierda A, Wong D, Stevens KA, Cascio S, Rossant J, and Zaret KS.** The formation and maintenance of the definitive endoderm lineage in the mouse: involvement of HNF3/forkhead proteins. *Development* 119: 1301–1315, 1993.
3. **Besnard V, Wert SE, Hull WM, and Whitsett JA.** Immunohistochemical localization of Foxa1 and Foxa2 during mouse development and in adult tissues. *Gene Expr Patterns* 5: 193–208, 2004.
4. **Bingle CD and Gitlin JD.** Identification of hepatocyte nuclear factor-3 binding sites in the Clara cell secretory protein gene. *Biochem J* 295: 227–232, 1993.
5. **Bingle CD, Hackett BP, Moxley M, Longmore W, and Gitlin JD.** Role of hepatocyte nuclear factor-3 alpha and hepatocyte nuclear factor-3 beta in Clara cell secretory protein gene expression in the bronchiolar epithelium. *Biochem J* 308: 197–202, 1995.
6. **Bohinski RJ, Di Lauro R, and Whitsett JA.** The lung-specific surfactant protein B gene promoter is a target for thyroid transcription factor 1 and hepatocyte nuclear factor 3, indicating common factors for organ-specific gene expression along the foregut axis. *Mol Cell Biol* 14: 5671–5681, 1994.
7. **Bolender RP, Hyde DM, and Dehoff RT.** Lung morphometry: a new generation of tools and experiments for organ, tissue, cell, and molecular biology. *Am J Physiol Lung Cell Mol Physiol* 265: L521–L548, 1993.
8. **Brown LA, Bliss AS, and Longmore WJ.** Effect of nutritional status on the lung surfactant system: food deprivation and caloric restriction. *Exp Lung Res* 6: 133–147, 1984.
9. **Cirillo LA, McPherson CE, Bossard P, Stevens K, Cherian S, Shim EY, Clark KL, Burley SK, and Zaret KS.** Binding of the winged-helix transcription factor HNF3 to a linker histone site on the nucleosome. *EMBO J* 17: 244–254, 1998.
10. **Clevidence DE, Overdier DG, Peterson RS, Porcella A, Ye H, Paulson KE, and Costa RH.** Members of the HNF-3/forkhead family of transcription factors exhibit distinct cellular expression patterns in lung and regulate the surfactant protein B promoter. *Dev Biol* 166: 195–209, 1994.
11. **Costa RH, Kalinichenko VV, and Lim L.** Transcription factors in mouse lung development and function. *Am J Physiol Lung Cell Mol Physiol* 280: L823–L838, 2001.
12. **Dave V, Childs T, and Whitsett JA.** Nuclear factor of activated T cells regulates transcription of the surfactant protein D gene (Sftpd) via direct interaction with thyroid transcription factor-1 in lung epithelial cells. *J Biol Chem* 279: 34578–34588, 2004.
13. **Duncan SA, Navas MA, Dufort D, Rossant J, and Stoffel M.** Regulation of a transcription factor network required for differentiation and metabolism. *Science* 281: 692–695, 1998.
14. **He Y, Crouch EC, Rust K, Spaite E, and Brody SL.** Proximal promoter of the surfactant protein D gene: regulatory roles of AP-1, forkhead box, and GT box binding proteins. *J Biol Chem* 275: 31051–31060, 2000.
15. **Ikeda K, Shaw-White JR, Wert SE, and Whitsett JA.** Hepatocyte nuclear factor 3 activates transcription of thyroid transcription factor 1 in respiratory epithelial cells. *Mol Cell Biol* 16: 3626–3636, 1996.
16. **Jobe AH, Newnham JP, Willet KE, Moss TJ, Gore Ervin M, Padbury JF, Sly P, and Ikegami M.** Endotoxin-induced lung maturation in preterm lambs is not mediated by cortisol. *Am J Respir Crit Care Med* 162: 1656–1661, 2000.
17. **Kaestner KH.** The hepatocyte nuclear factor 3 (HNF3 or FOXA) family in metabolism. *Trends Endocrinol Metab* 11: 281–285, 2000.
18. **Kaestner KH, Hiemisch H, Luckow B, and Schutz G.** The HNF-3 gene family of transcription factors in mice: gene structure, cDNA sequence, and mRNA distribution. *Genomics* 20: 377–385, 1994.
19. **Kaestner KH, Katz J, Liu Y, Drucker DJ, and Schutz G.** Inactivation of the winged helix transcription factor HNF3alpha affects glucose homeostasis and islet glucagon gene expression in vivo. *Genes Dev* 13: 495–504, 1999.
20. **Kelly SE, Bachurski CJ, Burhans MS, and Glasser SW.** Transcription of the lung-specific surfactant protein C gene is mediated by thyroid transcription factor 1. *J Biol Chem* 271: 6881–6888, 1996.
21. **Lai E, Prezioso VR, Smith E, Litvin O, Costa RH, and Darnell JE Jr.** HNF-3A, a hepatocyte-enriched transcription factor of novel structure is regulated transcriptionally. *Genes Dev* 4: 1427–1436, 1990.

22. **Li D, Gallup M, Fan N, Szymkowski DE, and Basbaum CB.** Cloning of the amino-terminal and 5′-flanking region of the human MUC5AC mucin gene and transcriptional up-regulation by bacterial exoproducts. *J Biol Chem* 273: 6812–6820, 1998.
23. **Lin Y and Lechner AJ.** Surfactant content and type II cell development in fetal guinea pig lungs during prenatal starvation. *Pediatr Res* 29: 288–291, 1991.
24. **Massaro D and Massaro GD.** Dexamethasone accelerates postnatal alveolar wall thinning and alters wall composition. *Am J Physiol Regul Integr Comp Physiol* 251: R218–R224, 1986.
25. **Massaro GD and Massaro D.** Formation of alveoli in rats: postnatal effect of prenatal dexamethasone. *Am J Physiol Lung Cell Mol Physiol* 263: L37–L41, 1992.
26. **Massaro GD, Radaeva S, Clerch LB, and Massaro D.** Lung alveoli: endogenous programmed destruction and regeneration. *Am J Physiol Lung Cell Mol Physiol* 283: L305–L309, 2002.
27. **McPherson CE, Shim EY, Friedman DS, and Zaret KS.** An active tissue-specific enhancer and bound transcription factors existing in a precisely positioned nucleosomal array. *Cell* 75: 387–398, 1993.
28. **Melton KR, Nesslein LL, Ikegami M, Tichelaar JW, Clark JC, Whitsett JA, and Weaver TE.** SP-B deficiency causes respiratory failure in adult mice. *Am J Physiol Lung Cell Mol Physiol* 285: L543–L549, 2003.
29. **Monaghan AP, Kaestner KH, Grau E, and Schutz G.** Postimplantation expression patterns indicate a role for the mouse forkhead/HNF-3 alpha, beta and gamma genes in determination of the definitive endoderm, chordamesoderm and neuroectoderm. *Development* 119: 567–578, 1993.
30. **Nijjar MS and Hatch GM.** Effects of premature weaning and diet on lung growth and appearance of adenylate cyclase activator in rat lung. *Mol Cell Biochem* 101: 59–66, 1991.
31. **Oshika E, Liu S, Ung LP, Singh G, Shinozuka H, Michalopoulos GK, and Katyal SL.** Glucocorticoid-induced effects on pattern formation and epithelial cell differentiation in early embryonic rat lungs. *Pediatr Res* 43: 305–314, 1998.
32. **Perl AK, Tichelaar JW, and Whitsett JA.** Conditional gene expression in the respiratory epithelium of the mouse. *Transgenic Res* 11: 21–29, 2002.
33. **Rausa FM, Tan Y, Zhou H, Yoo KW, Stolz DB, Watkins SC, Franks RR, Unterman TG, and Costa RH.** Elevated levels of hepatocyte nuclear factor 3beta in mouse hepatocytes influence expression of genes involved in bile acid and glucose homeostasis. *Mol Cell Biol* 20: 8264–8282, 2000.
34. **Ruiz i Altaba A, Cox C, Jessell TM, and Klar A.** Ectopic neural expression of a floor plate marker in frog embryos injected with the midline transcription factor Pintallavis. *Proc Natl Acad Sci USA* 90: 8268–8272, 1993.
35. **Sahebjami H and Domino M.** Effects of repeated cycles of starvation and refeeding on lungs of growing rats. *J Appl Physiol* 73: 2349–2354, 1992.
36. **Sasaki H and Hogan BL.** Differential expression of multiple fork head related genes during gastrulation and axial pattern formation in the mouse embryo. *Development* 118: 47–59, 1993.
37. **Sawaya PL and Luse DS.** Two members of the HNF-3 family have opposite effects on a lung transcriptional element; HNF-3 alpha stimulates and HNF-3 beta inhibits activity of region I from the Clara cell secretory protein (CCSP) promoter. *J Biol Chem* 269: 22211–22216, 1994.
38. **Shi SR, Key ME, and Kalra KL.** Antigen retrieval in formalin-fixed, paraffin-embedded tissues: an enhancement method for immunohistochemical staining based on microwave oven heating of tissue sections. *J Histochem Cytochem* 39: 741–748, 1991.
39. **Shih DQ, Navas MA, Kuwajima S, Duncan SA, and Stoffel M.** Impaired glucose homeostasis and neonatal mortality in hepatocyte nuclear factor 3alpha-deficient mice. *Proc Natl Acad Sci USA* 96: 10152–10157, 1999.
40. **Wan H, Dingle S, Xu Y, Besnard V, Kaestner KH, Ang SL, Wert S, Stahlman MT, and Whitsett JA.** Compensatory roles of Foxa1 and Foxa2 during lung morphogenesis. *J Biol Chem* 280: 13809–13816, 2005.
41. **Wan H, Kaestner KH, Ang SL, Ikegami M, Finkelman FD, Stahlman MT, Fulkerson PC, Rothenberg ME, and Whitsett JA.** Foxa2 regulates alveolarization and goblet cell hyperplasia. *Development* 131: 953–964, 2004.
42. **Wan H, Xu Y, Ikegami M, Stahlman MT, Kaestner KH, Ang SL, and Whitsett JA.** Foxa2 is required for transition to air breathing at birth. *Proc Natl Acad Sci USA* 101: 14449–14454, 2004.
43. **Wert SE, Yoshida M, LeVine AM, Ikegami M, Jones T, Ross GF, Fisher JH, Korfhagen TR, and Whitsett JA.** Increased metalloproteinase activity, oxidant production, and emphysema in surfactant protein D gene-inactivated mice. *Proc Natl Acad Sci USA* 97: 5972–5977, 2000.
44. **Whitsett JA, Wert SE, and Trapnell BC.** Genetic disorders influencing lung formation and function at birth. *Hum Mol Genet* 13*, Spec No* 2: R207–R215, 2004.
45. **Wikenheiser KA, Vorbroker DK, Rice WR, Clark JC, Bachurski CJ, Oie HK, and Whitsett JA.** Production of immortalized distal respiratory epithelial cell lines from surfactant protein C/simian virus 40 large tumor antigen transgenic mice. *Proc Natl Acad Sci USA* 90: 11029–11033, 1993.
46. **Zhou L, Dey CR, Wert SE, Yan C, Costa RH, and Whitsett JA.** Hepatocyte nuclear factor-3beta limits cellular diversity in the developing respiratory epithelium and alters lung morphogenesis in vivo. *Dev Dyn* 210: 305–314, 1997.